Diffusion and Performance of Fragranced Products: Prediction and Validation

Miguel A. Teixeira, Oscar Rodríguez, and Alírio E. Rodrigues
LSRE – Laboratory of Separation and Reaction Engineering, Associate Laboratory LSRE/LCM, Dept. of Chemical Engineering, Faculty of Engineering, University of Porto, Rua Dr. Roberto Frias, Porto 4200-465, Portugal

DOI 10.1002/aic.14106
Published online April 19, 2013 in Wiley Online Library (wileyonlinelibrary.com)

The design of fragranced products is a combination of art, technology, and scientific knowledge, although the former still predominates in the industry. For that reason, a theoretical model to assess their performance considering the release and diffusion together with the predicted odor intensity over time and distance from the source was developed and validated. Diffusion profiles were experimentally measured in a diffusion tube, similar to the Stefan tube, and predicted with a model for pure fragrance chemicals, binary, quaternary, and multicomponent (11 chemicals) mixtures. A very good agreement between our purely predictive model and experimental concentration data was observed. Fragrance concentrations in air were then converted into odor intensities using models from psychophysics, making it possible to evaluate the evolution of the odor with time and distance using a performance plot. Accordingly, the performance of these mixtures was modeled and experimentally validated, which constitutes a landmark for fragrance design. © 2013 American Institute of Chemical Engineers *AIChE J*, 59: 3943–3957, 2013
Keywords: perfume performance, fragrances, diffusion, release, odor perception

Introduction

If we put a bottle of one of the most renowned and finest perfumes on the shelf of a closed room and open up its cap, in the first moments we will not smell more than a brief and mild odor sensation. Initially, its odor will only be perceived near the source of release where its concentration is higher. Some hours later, we will smell it at some distance from the bottle. After a day or two, the whole room will have a homogeneous pleasant odor, characteristic of the main pattern of the perfume. However, fragrances along with their perception over time and distance are much more complex than it might look at a glance. The process governing this movement of fragrant molecules in the air is called diffusion. This phenomenon is typically slow, governing the overall rate of many processes occurring in Chemical Engineering.

However, in the real scenario of fragrances being released in air, it happens that when we apply a perfume it is often speeded up by convection phenomena (because we usually fan a paper blotter prior to smell it or a wind stream passes through an odor plume just after we apply it on our body). Despite that, the diffusion process alone may be described by two different approaches as stated by Cussler[1]: the more fundamental approach is based on Fick's law of diffusion by using diffusion coefficients, while the other approach would apply mass-transfer coefficients. The preference of one approach from the other is, according to Cussler, the result of a "*compromise between ambition and experimental resources*." If on one hand, it is desirable to follow a more fundamental perspective, diffusion coefficients should be preferred. But if a more approximate and phenomenological experiment is desired, such approximation would lead to mass-transfer coefficients.[1] In this work, we have followed the former perspective to develop a theoretical model that can be purely predictive.

For the specific case of fragrance release and propagation in air, the process of diffusion appears intimately interrelated with the evaporation mechanism, for which fragrance chemicals will play an important role. Altogether, they will influence the product's odor performance, consequently changing its acceptance from consumers. They are the ultimate judges for commercial fragranced products, and their preference will be mainly based on their sensory perception. This is so, because fragrance performance can be evaluated in terms of both perceived odor intensity and odor character at different distances from the source and over time (olfactory marketing is a new trend that highlights this fact). However, despite the relevance of this topic for the development of new products, the fact is that the industry often uses panels for sensory evaluation during the stages of idea generation and selection, within product design. Thus, at the scientific level there is little observed on the diffusion of fragrances. Note that the performance of fragranced products has been deeply studied by R&D departments of major fragrance houses, but that knowledge remains a trade secret. Although many of those use modeling tools to predict odor dispersion, they generally report only experimental measurements due to the difficulty of developing theoretical models for these phenomena. An overview of relevant works on the evaluation of the performance of perfumes is presented in Table 1.

Correspondence concerning this article should be addressed to A. E. Rodrigues at arodrig@fe.up.pt.

Table 1. Summary of Relevant Literature on the Performance of Fragrances

Approach	References
Definition of performance parameters like impact, tenacity, diffusion, volume, and substantivity, as well as important properties for the evaluation of performance like the odor value, odor threshold, or log P	2
Combination of headspace measurements with olfactometry data and correlation of physicochemical properties for evaluation of fragrance performance	3
Evaluation of perfume performance based on chemical structure related properties and physicochemical properties of the chemicals together with calculation of the perceived odor intensity	4
Enhancement of fragrance performance by encapsulating them into carrier materials using different techniques	5
Evaporation of fragrances from the human forearm under *in vivo* conditions considering evaporation and absorption rate constants and estimation of the release using physicochemical properties following nearly first-order kinetics Measurement and modeling of the evaporation rates of fragrance ingredients using dynamic headspace	6,7
Compositions of perfume mixtures to improve the release of fragrance materials from an entrapment structure on a surface over time	8
Prediction of the perceived odor of mixtures using the PTD® methodology and also of their performance in terms of time and distance using a model based on Fick's laws and performance parameters commonly used by the industry	9,10
Perfume compositions designed for use in wash-off systems to provide a high initial bloom with minimal residual perfume on the targeted system and a long sustained release of fragrance	11
Measurement of fragrance intensity above the skin using panelists and a labeled magnitude scale (LMS) for performance evaluation	12
Methods of formulating fragrance products to mask the malodor of ammonia	13
Proposal of perfume compositions comprising nonsubstantive fragrance materials in order to enhance product shelf life, delivery effectiveness and substantivity on different substrates	14
Modeling and experimental evaporation of multicomponent mixtures of 2–5 aliphatic and aromatic hydrocarbons, using a quantum chemical approach with COSMO-RS based CFD model	15

The aim of our study on the diffusion and performance of fragrances is to introduce some scientific knowledge into these phenomena using concepts from Chemical Engineering combined with psychophysics for human sensory perception. Within that point of view, it can be summarized at this time that perfumes can be considered as liquid solutions of fragrant components diluted in a suitable solvent (or a mixture of them, like ethanol and water). For their typical use, they are sprayed (e.g., on the skin or clothes), allowed to vaporize, and then diffuse through the surrounding space where they may be perceived by the people around. Chemical Engineering provides suitable models for vapor–liquid phase equilibria and gas diffusion, which can be used to describe these steps for the release of a fragrance into air. The concentration of odorants can then be translated into perceived sensations using models for odor intensity and odor perception, which can be taken from psychophysics. Altogether, this provides a suitable tool for describing and evaluating perfume behavior as we have shown in the recent past.[9,16–19] Such approach is within a new paradigm called Product Engineering, a branch inside chemical engineering which is focused on the design of new chemical, biological, or consumer products. Due to the diversity of natural and synthetic products, it encompasses different but interrelated scientific fields as it happens in this work for perfumed products with Chemical Engineering and psychophysics.[20–23]

Perfume structure, evaporation, and diffusion

A commercial perfume is a multicomponent mixture of fragrance chemicals (often, in the order of 50–100) with completely different physicochemical properties with respect to their molecular weight, vapor pressure, water solubility, octanol–water partitioning, polarity or odor detection threshold (ODT). Consequently, it is a complex homogeneous solution whose composition has been compared to a pyramidal structure which comprises top, middle, and base notes plus solvents and other chemicals.[2,24] Following this line of thought, it is expected that, theoretically, the perceived scent of a perfume that is evaporating and diffusing into the air should be evolving with time and changing through the surrounding space. In this way, top notes are considered the most volatile ones, and so should be more strongly perceived in the beginning, then the middle notes and, finally, after some hours, base notes will become more intense.[2] However, the fact is that this traditional view of the naturally occurring process of evaporation is too simplistic. It is purely a qualitative organoleptic analysis. Thus, depending on physical properties like the volatility of the fragrant molecules or the molecular interactions existing in the liquid, all fragrant species start to evaporate right after application of the perfume, but at different rates. Then, as the diffusion process takes place, a blend of fragrance vapors evolves in the air above the liquid and the human nose perceives them all simultaneously, though with different intensities each. Consequently, for a well-structured perfume, the perceived scent over time should be a perfect blend of notes as shown in Figure 1.

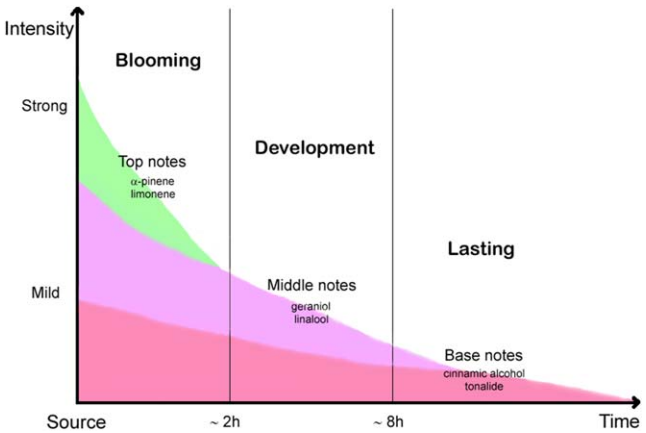

Figure 1. Simple perspective of the evaporation and perception of the different fragrant notes near the source of the perfume.

This is a representation of the behavior of typical top, middle, and base notes in a perfume. [Color figure can be viewed in the online issue, which is available at wileyonlinelibrary.com.]

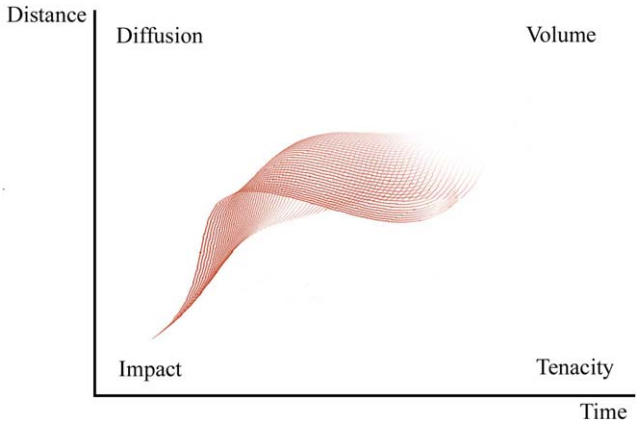

Figure 2. Parameters for the characterization of perfume performance as a function of time and distance: impact, tenacity, diffusion, and volume.

[Color figure can be viewed in the online issue, which is available at wileyonlinelibrary.com.]

Odor performance

Measuring the performance of a perfumed product is something complex. Perfumes may contain hundreds of chemical compounds in their composition. Moreover, it involves consumer perception and likeability. But, in other words, the performance of any kind of consumer product relies as the ultimate proof that it accomplishes the function for which it was made (e.g., that a deodorant masks the malodor of human body). According to Calkin and Jellinek,[2] the performance of a perfume is represented by its ability to become noticeable. Thus, performance enhancement starts in the optimization of product's composition, to obtain the maximum desired odor effect at the lowest possible concentration (once essential oils and fragrance chemicals can be quite expensive). Yet, several questions still remain to be unfolded: does the performance of a perfume depends on the intrinsic performance of its constituents? How should the performance of a perfumed product be measured and better yet, predicted?

In our approach, performance can be synthetically defined as the perceived odor intensity (quantitative measure) and character (qualitative measure) over time and distance from the source of release. The perfumery industry defined a set of performance parameters that are of value to account for fragrance release and propagation, namely: impact, tenacity, diffusion, and volume. During the perfume formulation process, perfumers (the experts in the design of perfumes) seek to optimize these parameters that are schematically represented in Figure 2. Impact represents an immediate olfactory sensation, diffusion refers to the efficacy of a perfume at some distance from the source, tenacity is the performance index that measures the persistence of a fragrance for long times after its application but near the evaporating source, and finally, volume is the effectiveness of a perfume over distance, some time after application.[4,10,25] Here, we will follow our methodology using these four performance parameters together with the diffusion model as presented elsewhere.[9,26]

The objective of this work is to present and validate experimentally a suitable model for the prediction of fragrance release and diffusion which will, ultimately, allow the evaluation of the performance of fragranced products. To do so, the diffusion profiles of fragrances in air were experimentally measured and compared with simulations from a purely predictive model. Diffusion studies were performed for ethanol (solvent), α-pinene (top note), a binary mixture of them, a quaternary mixture (α-pinene + linalool + tonalide + ethanol) which involves top, middle, and base notes with a solvent. Furthermore, it was applied to a complex multicomponent mixture with 11 compounds for the first time (see Table 2).

Methodology

Perfume diffusion model

To characterize the release and propagation of fragrance chemicals in air, the physical system considered in this work is very similar, in phenomenological terms, to the classic Stefan tube problem.[31–34] This is expressed by a liquid i that evaporates into a stagnant gas film j with a gas stream of air at the top as depicted in Figure 3. This gas stream is passed at a rate sufficient to assume the concentration of the diffusing gas as zero but low enough and with the correct orientation to prevent turbulence inside the tube.

Table 2. Properties of the Fragrance Chemicals Obtained from the Literature

Fragrance Chemical	P^{sat} (Pa)[a]	MW (g/mol)[b]	ODT (g/m^3)[c]	n_i[d]	ρ (g/mL)[b]	$D_{i,air}$ (m^2/h)[e]
α-pinene	513.4[f]	136.13	2.40 E-04	0.49	0.879	2.17×10^{-2}
Limonene	205.4[f]	136.13	6.19 E-04	0.37	0.841	2.17×10^{-2}
Decanal	27.6[b]	156.15	9.92 E-06	0.39	0.830	2.07×10^{-2}
Linalool	22.1[f]	154.14	9.26 E-06	0.35	0.858	2.10×10^{-2}
Benzyl Acetate	21.86[f]	150.07	3.32 E-04	0.38	1.055	3.73×10^{-2}
Geraniol	2.67[b]	154.14	9.01 E-06	0.36	0.867	2.10×10^{-2}
2-Phenethyl Alcohol	9.87[b]	122.07	1.80 E-05	0.34	1.020	4.64×10^{-2}
Cinnamic Alcohol	1.6[b]	134.07	2.74 E-07	0.34	1.049	3.95×10^{-2}
Tonalide	0.00007[b]	258.4	1.82 E-05	0.34	0.919	1.92×10^{-2}
Ethanol	7050[f]	46.04	1.21 E-01	0.58	0.789	4.42×10^{-2}
Deionized Water	0.00317[b]	18.15	–	–	1.000	9.13×10^{-2}

Vapor Pressure at (P^{sat}), Molecular Weight (MW), Odor Detection Threshold (ODT), Olfactory Power Law Exponent (n_i, nondimensional), Density (ρ) and Molecular Diffusivity in Air ($D_{i,air}$)

[a]vapor pressures for pure components were obtained at 296.15 K.

[b]From Chemspider Database.[27]

[c]ODTs were geometrically averaged from data available in van Gemert, L.J.[28]

[d]From Devos et al.[29]

[e]Estimated from Fuller et al.[30]

[f]From DIPPR 801 Database.

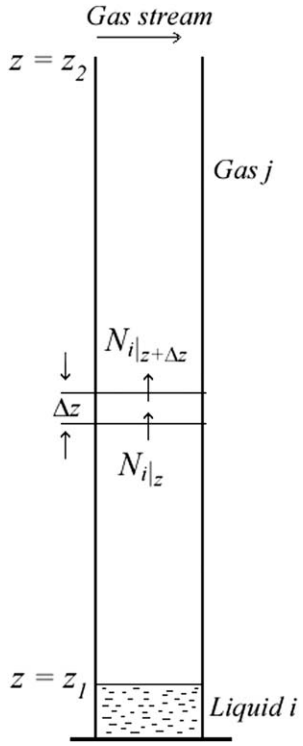

Figure 3. Schematic representation for the diffusion of species *i* through a stagnant fluid *j* (similar to the Stefan tube).

The solution of Fick's first law as a function of the molar flux relative to stationary coordinates for a single component can be presented as follows[35]

$$N_{i,z} = -c_T D_{ij} \frac{\partial y_i}{\partial z} + y_i \left(N_{i,z} + N_{j,z}\right) \tag{1}$$

where $N_{i,z}$ is the number of moles of component i that go through the unit area per unit of time (molar flux), being the unit area fixed in space. c_T is the total concentration, D_{ij} is the diffusion coefficient of species i in species j, y_i is the vapor mole fraction of i, $N_{j,z}$ is the corresponding flux for species j and z is the flux direction. If a steady-state condition is assumed and species j (in this case, air) is considered as a stagnant fluid ($N_{j,z} = 0$), then Eq. 1 can be rewritten as

$$N_{i,z} = \frac{-c_T D_{ij}}{1-y_i} \frac{dy_i}{dz} \tag{2}$$

Moreover, performing a mass balance to the volume element depicted in Figure 3 at steady-state conditions, $dN_i/dz = 0$, then Eq. 2 can be expressed as

$$\frac{dN_{i,z}}{dz} = \frac{d}{dz}\left(\frac{c_T D_{ij}}{1-y_i} \frac{dy_i}{dz}\right) = 0 \tag{3}$$

From this point, if we assume ideal solution in the gas phase, T and P constant, D_{ij} independent of the concentration, and c_T a constant factor, it is possible to integrate Eq. 3 which results into Eq. 4 as defined by Bird, Stewart, and Lightfoot (BSL model)[35]

$$\left(\frac{1-y_i}{1-y_{i,1}}\right) = \left(\frac{1-y_{i,2}}{1-y_{i,1}}\right)^{\frac{z-z_1}{z_2-z_1}} \tag{4}$$

where z_1 and z_2 are the positions at the interface and at the end of the tube, while $y_{i,1}$ and $y_{i,2}$ are the corresponding vapor mole fractions of i.

Thus, from Eq. 4, it is possible to calculate the steady-state concentration profile inside the tube for a fragrant species that is diffusing upward.

On the other hand, if we recall Eq. 2 and seek for an unsteady state solution (transient state), then the mass balance to the volume element is given by $-\partial N_i/\partial z = \partial C_i/\partial t$, and it can be written that

$$-\frac{\partial N_{i,z}}{\partial z} = \frac{\partial}{\partial z}\left(\frac{c_T D_{ij}}{1-y_i} \frac{\partial y_i}{\partial z}\right) = c_T \frac{\partial y_i}{\partial t} \tag{5}$$

which by derivation gives

$$\frac{\partial y_i}{\partial t} = \frac{D_{ij}\left[\left(\frac{\partial y_i}{\partial z}\right)\left(\frac{\partial y_i}{\partial z}\right) + (1-y_i)\frac{\partial^2 y_i}{\partial z^2}\right]}{(1-y_i)^2} \tag{6}$$

Equation 6 gives the concentration profile of a fragrance i as a function of time (t) and distance (z) inside the tube. Even so, we need to relate this concentration with that of the liquid perfume. This can be done by mass balance through the liquid–gas interface, as described by

$$\frac{dn_i}{dt} = \frac{D_{ij} A_{gl}\, c_T}{1-y_i} \frac{\partial y_i}{\partial z}\Big|_{z=0} \tag{7}$$

Equations 6 and 7 provide a system of two differential equations for each volatile component in the perfume. This has to be solved with the following initial (IC) and boundary conditions (BC)

$$\text{I.C.} \quad t=0, \quad (z=0) \quad n_i = n_{i,0} \tag{8}$$

$$\text{B.C.} \quad t>0, \quad z=0 \quad y_i = y_{i,eq} = \left(\frac{\gamma_i P_i^{sat} x_i}{P}\right) \tag{9}$$

$$z = z_{max} \quad y_i = 0 \tag{10}$$

where n_i is the number of moles of component i and $n_{i,0}$ is the initial number of moles of component i in the liquid solution while y_i is the mole fraction of component i and $y_{i,eq}$ is the mole fraction of component i in the gas phase in equilibrium with that of the liquid which is traduced by x_i. Additionally, γ_i is the activity coefficient in the liquid phase, P_i^{sat} is the saturated vapor pressure for component i, P is the total pressure in the system and z_{max} represents the maximum distance in the axial coordinate.

In this way, initial condition represented by Eq. 8 is related to the perfume formulation, and the lower-end boundary condition specified by Eq. 9 includes the evaporation model, here a modified Raoult's Law. Activity coefficients were calculated by means of the UNIFAC method.[36]

Numerical solution

The solution of the coupled Eqs. 5 and 6 together with initial and boundary conditions gives the concentration profiles over time for each species in the unsteady regime. Both approaches, steady state and unsteady state, were used for the modeling of the fragrance systems considered here. The resolution of the coupled system(s) of equations (ODE + PDE) was performed in Matlab® using the *pdepe* package for numerical computation of partial differential

equations (PDE). This routine solves initial-boundary value problems for systems with parabolic and elliptic PDEs in one space variable *(z)* and time *(t)*.[37] The calculations over the space variable include second-order approximations to the solution on the specified space mesh. The ordinary differential equations (ODE) resulting from the discretization in space were integrated using the *ODE15s* solver package to obtain the approximate solutions over time *(t)* using relative and absolute tolerances of 10^{-8}. This solver is based on the numerical differentiation formulae which are implemented with backward differences. These are generally more efficient than the backward differentiation formulas, although for higher orders they are less stable.[38] Moreover, the solver uses the method of finite differences for the discretization of the space variable using 254 elements.[39–41]

Odor perception model

Once we have computed the concentrations in the gas phase for each fragrance chemical, it is necessary to convert them into odor intensities as perceived by our nose. For that purpose, we can recall psychophysics, a science within psychology that deals with the mathematical relationships between a stimulus magnitude and its perceived sensation. Among these models, Stevens' Power Law for olfaction[19,42] defines the odor strength or intensity of an odorant i (ψ_i) as the ratio between its concentration in the headspace (C_i^g) and its ODT in air (ODT_i), raised to an exponent (n_i) as presented in Eq. 11

$$\psi_i = \left(\frac{C_i^g}{ODT_i}\right)^{n_i} \tag{11}$$

where both concentration variables are in g/m^3, and the ODT defines the minimum concentration of an odorant that can be detected by the human nose.[2,43] Furthermore, when considering a perfume mixture with N fragrance chemicals, it is expected that N different odor intensities can be calculated in the headspace. To account for the odor character of such mixtures, the stronger component model can be used. It states that the odor intensity of the mixture is approximately equal to the maximum odor intensity of its components. Besides, this component with the maximum odor intensity will also be more strongly perceived and recognized by the human nose, although there is a mixture of perceived scents in air[44,45]

$$\psi_{mix} = \max\{\psi_i\}, \qquad i = 1, ..., N \tag{12}$$

For further details on the application of this odor perception model, we recommend the interested reader to follow our previous works.[9,16,18,26]

Materials and Methods

Materials

(−)-α-pinene (CAS #7785-26-4, >98%, purum), decanal (CAS #112-31-2, >95%, GC), and (±)-linalool (CAS #78-70-6, >97%, GC) were supplied by Fluka. R-(+)-limonene (CAS #5989-27-5, >97%, >98%, ee), geraniol (CAS #106-24-1, >98%), benzyl acetate (CAS #140-11-4, >99%), 2-phenylethanol (CAS #60-12-8, >99%, FCC, FG), and cinnamic alcohol (CAS #104-54-1, 98%, GC) were supplied by Sigma-Aldrich. Tonalide (CAS # 21145-77-7) was purchased from Aroma & Fine Chemicals. Ethanol (Absolute GR for analysis, >99.9%) was supplied by Merck and deionized water ($\sigma < 2$ μS/cm) was produced in the LSRE laboratory using a two-column system of packed ion exchange resins. All reagents were used as received without further purification. Some relevant physicochemical properties of these components are presented in Table 2. Molecular diffusivities were calculated from the method of Fuller et al.[30,36], which is known to yield the smallest average errors among many other methods (for further details on their calculation see Refs. 9 and 36).

Experimental diffusion profiles

A diffusion tube 2 m long with five sampling ports (SP) positioned at different heights from the gas–liquid interface which is located at its bottom was designed and is presented in Figure 4. The diffusion tube was constructed with a constant nominal pipe size of 1, corresponding to an internal diameter of 2.41 cm (from the top to the bottom including the conical section to screw in the sample glass vessel). The tube was made of stainless steel and jacketed in case nonambient temperature is required. The SPs are positioned at distances of 0.13, 0.38, 0.63, 1.13, and 1.63 m from the gas–liquid interface, and were also made of stainless steel. These parts consisted of perforated pieces for screwing in the tube and were designed to tighten a PTFE/silicone septum that is flanked by two perforated rings of PTFE with a central diameter hole of 2 mm. Such rings were used in both sides of the septum to increase contact area and eliminate leaks. Moreover, at the top of the diffusion tube a sweep fan was placed to make the concentration null at that point.

For the measurement of fragrance diffusion profiles, a volume of 1 mL of solution (pure chemicals or mixtures of them) was pipetted and placed inside the glass vessel presented in Figure 4c. The start of each experiment was considered when the glass vessel was placed in the diffusion tube. For the case of fragrance mixtures, they were prepared gravimetrically using a Mettler Toledo balance model AB265-S with a precision of ± 0.2 mg. The liquid mixture was allowed to evaporate and diffuse upward (1-dimensional diffusion) and samples were being collected over time from the different SPs, using gas-tight syringes (SGE and Hamilton, see details ahead). Samples were then injected in a gas chromatograph (GC) with flame ionization detector for quantification. All experiments were run at room temperature (23 ± 1°C), controlled through an air-conditioning system. Vapor compositions were determined by headspace gas chromatography, using a Varian CP-3800 equipped with a split/splitless injector and a capillary column Chrompack CP-Wax 52 CB, 50 m length, 0.25 mm i.d., 0.2 μm film thickness. For the case of ethanol and α-pinene, the oven temperature was programmed isothermal at 60°C for 7 min only. For mixtures, it was set at 90°C for 7 min, then heated up to 160°C at a heating rate of 20°C/min, held isothermal for 7 min, then heated up to 220°C at a heating rate of 20°C/min, and finally held isothermal for 9.5 min. The injector and detector ports were set at 240 and 250°C, respectively. Injection volume for the gas phase was 0.1 or 0.25 mL with a split ratio of 1:5. Injection was performed using gas-tight syringes from SGE and Hamilton pressure lock of 0.100 and 0.250 mL. The carrier gas was helium (He N60) with a constant flow rate of 1.2 mL/min. Calibration

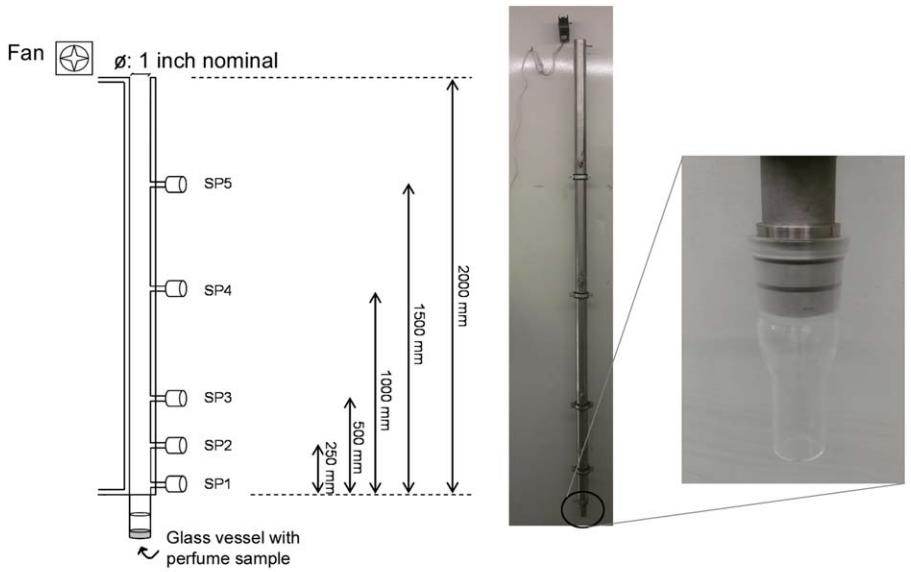

Figure 4. Schematic representation of the projected diffusion tube (a), photograph of the system in the lab (b) and of the glass vessel for the sample (c).

[Color figure can be viewed in the online issue, which is available at wileyonlinelibrary.com.]

lines were obtained for the pure components analyzed in triplicate. For that purpose, GC operating conditions were the same as for the samples.

Results and Discussion

The modeling of the diffusion process was performed considering the fundamental approach based on the Fick's law for diffusion. However, as previously said, there could be a preference for mass-transfer coefficients. We consider that the former is more appropriate for our study as we are dealing with (fragrance) concentrations measured over time and distance, instead of dealing with average concentrations (as happens with mass-transfer coefficients). Moreover, this choice allows the development of a predictive model, as diffusion coefficients can be predicted by suitable methods (e.g., Fuller et al.). Furthermore, a typical phenomenon that happens in many Chemical Engineering problems involving diffusion across an interface is that the resistance to mass transfer in the gas phase is often neglected. Here, a parenthesis is made to investigate this question. First, the geometry and volume of liquid play an important role. Thus, considering the particular "geometry" resulting from perfume spray, which is the case considered here, it is possible to do some rough calculations to evaluate the resistance to mass transfer both in the liquid and gas phases, as follows: the mass-transfer coefficient is defined as $k = D/\delta$ where D is the diffusion coefficient (m^2/s) and δ is the film thickness (m).[46,48] Typical values for these parameters are presented in Table 3.

Table 3. Typical Values for Molecular Diffusivity (D) and Film Thickness (δ) for Gases and Liquids

	Gas	Liquid
D (m^2/s)[a]	$(10^{-4}$ to $10^{-6}) \sim 10^{-5}$	$(10^{-8}$ to $10^{-10}) \sim 10^{-9}$
δ (m)[b]	$10^{-3}-10^{-4}$	$10^{-4}-10^{-5}$[c]

[a]From Perry and Green[46] and Bird, et al.[47]
[b]From Taylor and Krishna[48]
[c]E.L. Cussler in *"Diffusion: Mass transfer in fluid systems,"*[1] recommends a value of $\delta = 10^{-4}$ for liquids.

The mass-transfer coefficients in the gas (k_g) and liquid phases (k_l) are then calculated as $k_g = 10^{-1} - 10^{-2}$ m/s and $k_l = 10^{-4} - 10^{-5}$ m/s, respectively. These are in good agreement with the mass-transfer coefficients published by Wesselingh and Krishna,[49] reported as $k_g = 10^{-1}$ m/s and $k_l = 10^{-4}$ m/s.

Now, the overall mass-transfer coefficient, assuming a linear model for the description of the vapor–liquid equilibrium (VLE) can be given by

$$\frac{1}{k_{\mathrm{Tot}}} = \frac{1}{k_g} + \frac{1}{k_l}\frac{c_g^{\mathrm{T}}}{c_l^{\mathrm{T}}}K_i \tag{13}$$

with k_{Tot} as the overall mass-transfer coefficient and K_i as the equilibrium ratio ($y_i = K_i\ x_i$), while c_g^{T} and c_l^{T} are the total concentrations in gas and liquid phases, respectively.

The ratio of gas to liquid concentrations can be computed for some of the perfume mixtures presented in this work (e.g., α-pinene + linalool + tonalide + ethanol) near the interface at initial times after evaporation has started. For this case it was obtained a ratio of concentrations as:

$$\frac{c_g^{\mathrm{T}}}{c_l^{\mathrm{T}}} = \frac{6.23\times10^{-1}\ \mathrm{mol/m^3}}{5.57\times10^{3}\ \mathrm{mol/m^3}} = 1.12\times10^{-4} \tag{14}$$

Moreover, the equilibrium ratios, K_i, can be determined using the UNIFAC method in a modified Raoult's law (see Eq. 9). Considering the case of α-pinene near the interface for relatively short times after the evaporation process takes place, it is obtained that

$$\begin{cases} K_i = \dfrac{y_i}{x_i} = \dfrac{2.74\times10^{-3}}{2.74\times10^{-1}} \approx 10^{-2} & \text{at } t = t_0 = 0\,\mathrm{s} \\ K_i = \dfrac{y_i}{x_i} = \dfrac{2.74\times10^{-3}}{2.75\times10^{-1}} \approx 9.9\times10^{-3} & \text{at } t = 16\,\mathrm{s} \end{cases} \tag{15}$$

Additionally, initial values of the equilibrium ratios for the other fragrance chemicals in this quaternary mixture are presented in Table 4.

Table 4. K_i Values for the Different Fragrance Chemicals in the Quaternary Mixture of α-pinene + linalool + tonalide + ethanol

t (s)	K_i (α-pinene)	K_i (Linalool)	K_i (Tonalide)	K_i (Ethanol)
0	1.00×10^{-2}	3.33×10^{-4}	2.58×10^{-9}	1.12×10^{-1}
16	9.99×10^{-3}	3.34×10^{-4}	2.58×10^{-9}	1.12×10^{-1}

Using the values presented above, it is possible to estimate the resistance to mass transfer in the gas and liquid phases, respectively, considering the case of α-pinene

$$\frac{1}{k_g} \cong 10; \frac{1}{k_l} \cong 10^4; \text{ and } \frac{1}{k_l}\frac{c_g^T}{c_l^T}K_i \cong K_i \cong 10^{-2} \quad (16)$$

Similar results can be obtained for other compounds. In this way, with a simple calculation, it can be said that the resistance to mass transfer in the gas phase would exceed that in the liquid phase. Thus, the choice for diffusion coefficients is justified. However, note that for a different geometry (as a bottle of perfume with a larger volume of liquid), opened and evaporating into the atmosphere, it may be reasonable to consider the approach using mass-transfer coefficients.

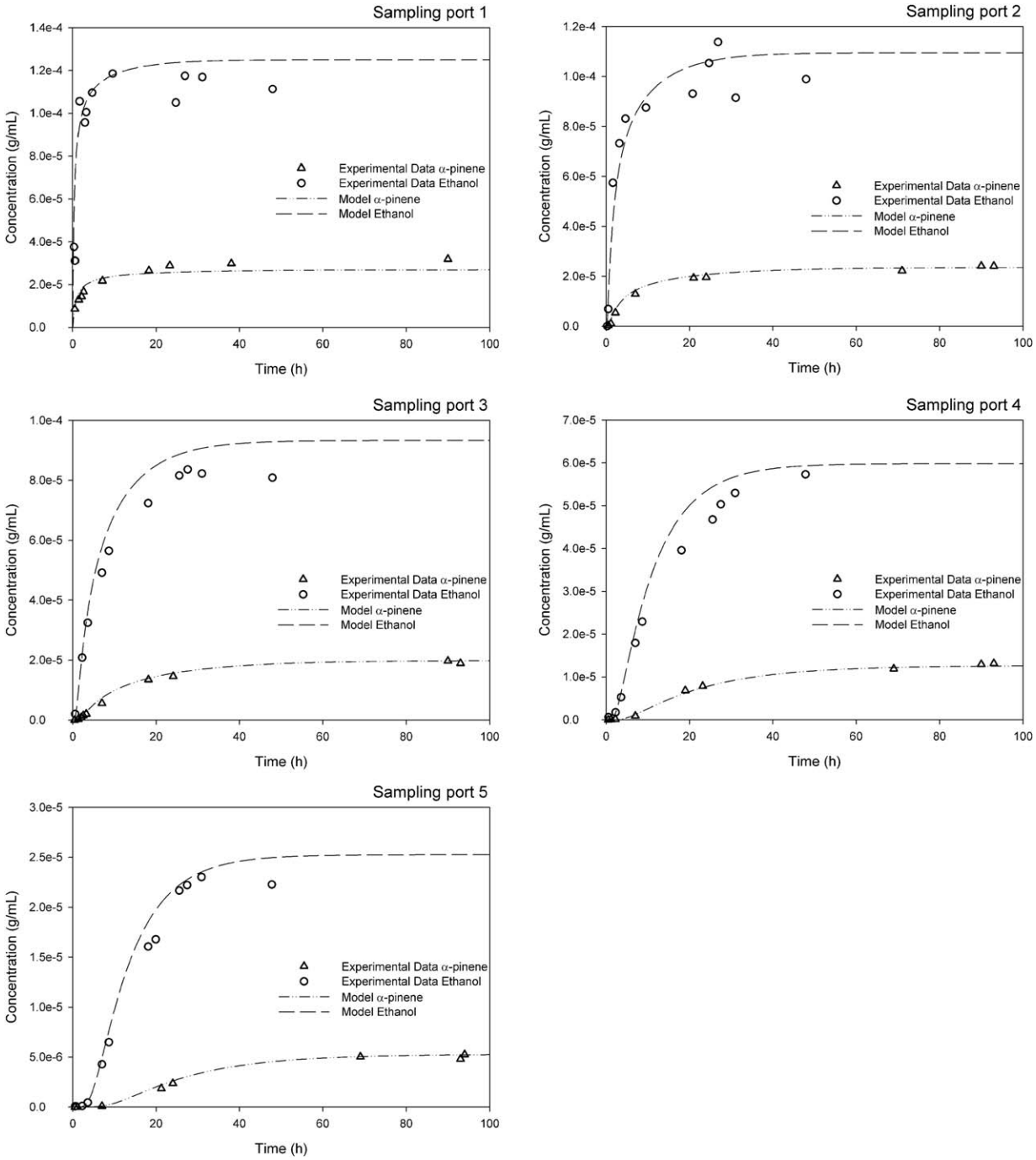

Figure 5. Experimental data (open symbols) and modeling (dashed lines) for the diffusion of pure components in air (ethanol - circles, α-pinene - triangles) measured at different heights from the source (different SPs).

Table 5. Average Relative Deviations (ARD, %) and Number of Data Points (*N*) for the Experimental Data Measured in the Diffusion Tube in All Experiments

	ARD (%)	N
Single chemical		
α-pinene	9.4	38
ethanol	11.4	45
Binary mixture		
α-pinene	16.9	46
ethanol	12.2	53
Quaternary mixture		
α-pinene	14.1	24
ethanol	3.2	27
Multicomponent mixture		
α-pinene	9.2	40
ethanol	13.5	42
limonene	21.9	43
Overall	12.8	358

Diffusion of pure fragrance chemicals

Recalling Eq. 1 for Fickian diffusion, it should be noted that, more than a century ago, Fick faced difficulties proving its validity throughout experiments with salt solutions.[50] Nevertheless, he did succeed in performing experiments at the steady-state regime. Similarly, in this study the measurement of diffusion profiles was first performed for pure components till they reached the steady state. Concentration profiles were obtained for ethanol and α-pinene using the conditions described before. The experimental data were compared with those obtained from our model (Eqs. 5 and 6) and also with the steady-state condition defined by Eq. 4. These concentration profiles are presented in Figure 5 for both components (although experiments were run for single species). Different SPs are shown separately, due to the differences in magnitude of concentrations. The average relative deviations (ARD, %) for all the diffusion experiments are shown in Table 5.

It is to be noted that our purely predictive model fits well with the experimental data for ethanol at short times ($\leq$10 h). This means that the estimated diffusion coefficient for ethanol can be acceptable. As indicated above, diffusion coefficients in air were estimated by the method of Fuller et al.[30] at 296 K (23°C), and for ethanol it was equal to $D_{\text{ethanol,air}} = 4.469 \times 10^{-2}$ m^2/h. This value compares favorably with those experimentally measured at 298 K by Wilke and Lee[31] and Lugg[51] which were 4.860×10^{-2} and 4.252×10^{-2} m^2/h, respectively. The correlation of Fuller et al. is considered as one of the methods with lower associated errors and the estimated diffusion coefficient is expected to be within an error of 5.4%, as reported in the literature.[30,36] Moreover, the steady-state concentrations were fairly well predicted by the model when compared to experimental data, although they tend to be slightly over predicted. The concentrations of ethanol determined on the long run (steady-state concentrations measured in the different *plateaus* observed in Figure 5) can be used to trace the concentration profile of ethanol as a function of the distance from the source of release. Experimental values were measured after more than 30 h from the beginning of the run and a comparison is also performed using the prediction from Eq. 4 (BSL model) for steady-state and the nonsteady-state simulation computed in Matlab®. The experimental measurements presented in Figure 6 (left) are the result of averaged values from several determinations and so the standard deviation is also presented as error bars.

Experimental errors should be taken into consideration, especially because when measuring extensive properties (the mass of an odorant inside the gas-tight syringe), great care should be taken in the sampling procedure. In this way, an imperfect sampling or a slight variation of the collected volume in the gas-tight syringe by the researcher might lead to differences in the concentration measured by GC. Consequently, it is seen that for sampling port 5, the measured vapor concentration is very close to the prediction, although for the remaining ports these were lower. Nevertheless, relative deviations between the measured and predicted steady-state concentrations were of 7.8, 8.4, 15.3, 12.6, and 11.8%, for SP 1, 2, 3, 4, and 5, respectively. Finally, it should be said that the solution obtained from the algebraic Eq. 4 gives the same result as the coupled Eqs. 5 and 6 once those lines appear superposed in Figure 6.

Diffusion experiments were also performed for α-pinene using the same conditions, techniques, and protocol as for the experiments with ethanol. The experimental data for the concentration profiles of α-pinene in the diffusion tube are

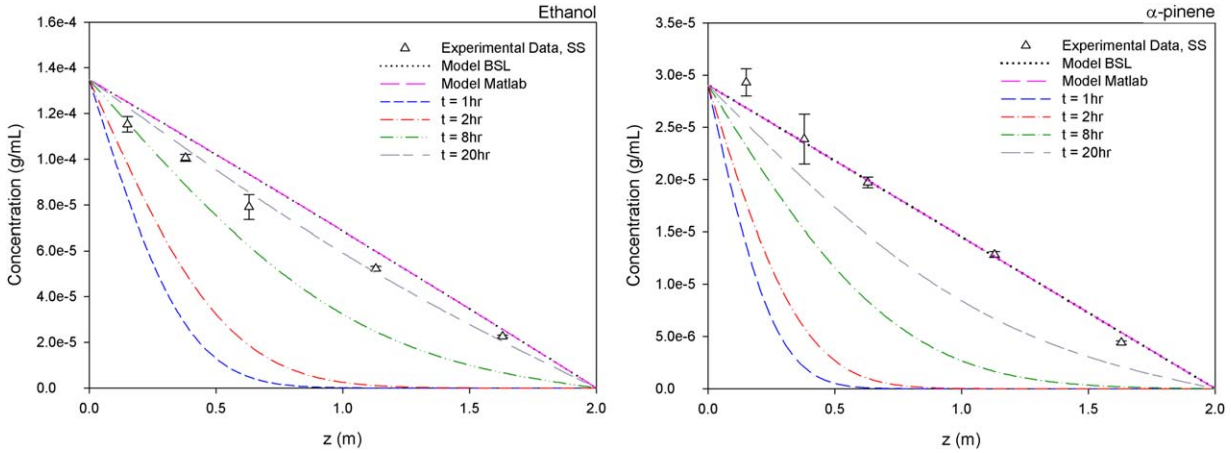

Figure 6. Experimental data (open triangles) for the steady-state concentrations measured at different heights for ethanol (left) and α-pinene (right), and simulations using Eq. 4 (BSL model) and the coupled Eqs. 5 and 6 (Model Matlab).

[Color figure can be viewed in the online issue, which is available at wileyonlinelibrary.com.]

presented in Figure 5 as well, for each sampling port together with the predicted model. The average relative deviation (ARD, %) is shown in Table 5. These experiments were performed for longer times (~100 h) than ethanol because α-pinene is also less volatile. A good agreement between experimental data and the model is observed for concentration profiles of α-pinene, except for sampling port 1 where the steady-state concentration is under predicted. For this sampling port, placed close to the interface, it should also be noted that after 1 and 50 h vapor concentrations reached nearly 50 and 99% of that measured at the stationary *plateau* while for sampling port 5, it was 0 and 87%, respectively. This shows the slow rate of the diffusion process alone. Moreover, it is seen that the predicted diffusion profiles on the different SPs fit well with the experimental data for short times, thus showing again that the diffusion coefficient estimated for α-pinene in this study is satisfactory.

The concentrations for α-pinene measured on the long run (≥90 h) and averaged from several measurements can be used to plot its corresponding concentration profile as a function of the distance from the source of release, as shown in Figure 6 (right). In this case, relative deviations for the different SPs 1, 2, 3, 4, and 5 were found to be 9.1, 1.4, 1.0, 1.7, and 13.3%, respectively. Thus, it is possible to see that, with the exception of sampling port 5, average errors are below 10% and so there is a good agreement between the experimental steady-state concentrations and those predicted by the model.

Diffusion of a binary mixture

On the other hand, diffusion experiments for the binary system of ethanol and α-pinene were also studied using a mixture with a molar composition of $x_{\text{ethanol}} = 0.891$ and $x_{\alpha\text{-pinene}} = 0.109$. The experimental data together with the modeling for the concentration profiles of both components using Eqs. 5 and 6 for the transient diffusion is presented in Figure 7.

First, it can be observed that ethanol presents significantly higher concentrations in air than α-pinene at all times and distances from the source. This behavior was expected due to its higher concentration in the mixture but also a much higher vapor pressure and diffusivity than α-pinene (see Table 2, as well as data for pure component experiments). Moreover, it can be said that this experimental methodology allows the measurement of the concentration profiles over time and distance with fair accuracy, although deviations may be found for some experimental points (once again, ethanol concentrations on the long run, >20 h, are slightly over predicted). The ARDs (%) calculated for ethanol and α-pinene were of 12.2 and 16.9% as shown in Table 5.

It is important to note that the composition of the mixture changes with time, and so the concentration of the vapor in equilibrium (boundary condition) is also evolving with time (except if an azeotrope is reached). Thus, for mixtures a steady state is never attained and so Eq. 4 does not apply.

Diffusion of quaternary mixtures

The diffusion of a quaternary fragrance system composed by α-pinene (top note) + linalool (middle note) + tonalide (base note) + ethanol (solvent) was studied. For that purpose, it was intended to evaluate the effect of the base note (which in this case is a fixative) on the release of the most volatile components. Tonalide was chosen as the base note for this mixture due to its fixative effect, easiness in experimental handling, and also for the availability of parameters for prediction of the VLE. In this way, the diffusion of two quaternary mixtures (Q1 and Q2) with a similar composition but differing in tonalide content was evaluated. These mixtures present an analogous composition in a tonalide free-basis, as shown in Table 6. The diffusion profiles in sampling port 1 are shown in Figure 8 for ethanol and α-pinene only, because the concentrations of linalool and tonalide in the gas phase were very low and below the detection limit of the GC. The ARDs (%) calculated for ethanol and α-pinene are given in Table 5.

The predicted diffusion profiles for the most volatile components in both quaternary mixtures fit well with the experimental data. An initial increase and dominance in the concentration of ethanol is observed, but as it vanishes in the liquid its concentration in the gas phase decreases with time. Nevertheless, it is important to highlight here the verification of the fixative effect of tonalide on the most volatile species: it is seen that for mixture Q2 (rich in tonalide) the maximum measured concentrations for ethanol and α-pinene are lower than for mixture Q1. The effect is more relevant for ethanol (maximum concentration in Q1 is the double of Q2 mixture) than for α-pinene, probably due to the latter being far less polar. Moreover, the concentration of α-pinene exceeds that of ethanol in a shorter period of time than for Q1, showing that tonalide has a higher retention effect on ethanol (polar molecules).

Diffusion of multicomponent perfume

To get closer to a real perfume formulation, a multicomponent mixture comprising different top, middle, and base notes plus an alcohol/water solvent was formulated. Such formulation pretended to mimic a typical composition of an e*xtrait* or *parfum*, considering its concentration ranges for ethanol, water, and perfume concentrate (for further details on this topic see Refs. 2 and 18). It should be highlighted that such formulation must obey some rules in terms of composition and selection of fragrance raw materials to have a homogeneous mixture with a pleasant smell evolving through time (e.g., fragrance chemicals are typically highly insoluble in water, but water must be used in perfume formulation to reduce alcohol perception). The selection of the fragrance chemicals and the corresponding composition was based on the expertise of the team on fragrance design. This formulation comprised different types of fragrances covering top, middle, and base notes as presented in Table 7. Note, however, that in the literature, multicomponent mixtures most often refer to ternary and, sometimes, quaternary mixtures only. Here, we made an effort to go a step forward to get closer to a real perfume formulation (50–100 components). It should be highlighted that the experimental determination of diffusion profiles for multicomponent mixtures is a difficult task. This is due to the difficulty of optimizing the experimental procedure to minimize the propagation of errors, even more when we are dealing with chemicals like fragrances which present large differences in volatility. Altogether, these are some of the reasons why this is the first study ever showing results for the performance of multicomponent mixtures of up to 11 chemicals.

The concentration and odor intensity profiles for ethanol, α-pinene and limonene, which are the most volatile compounds used in the formulation, are shown in Figure 9 for the different SPs. All other components could not be

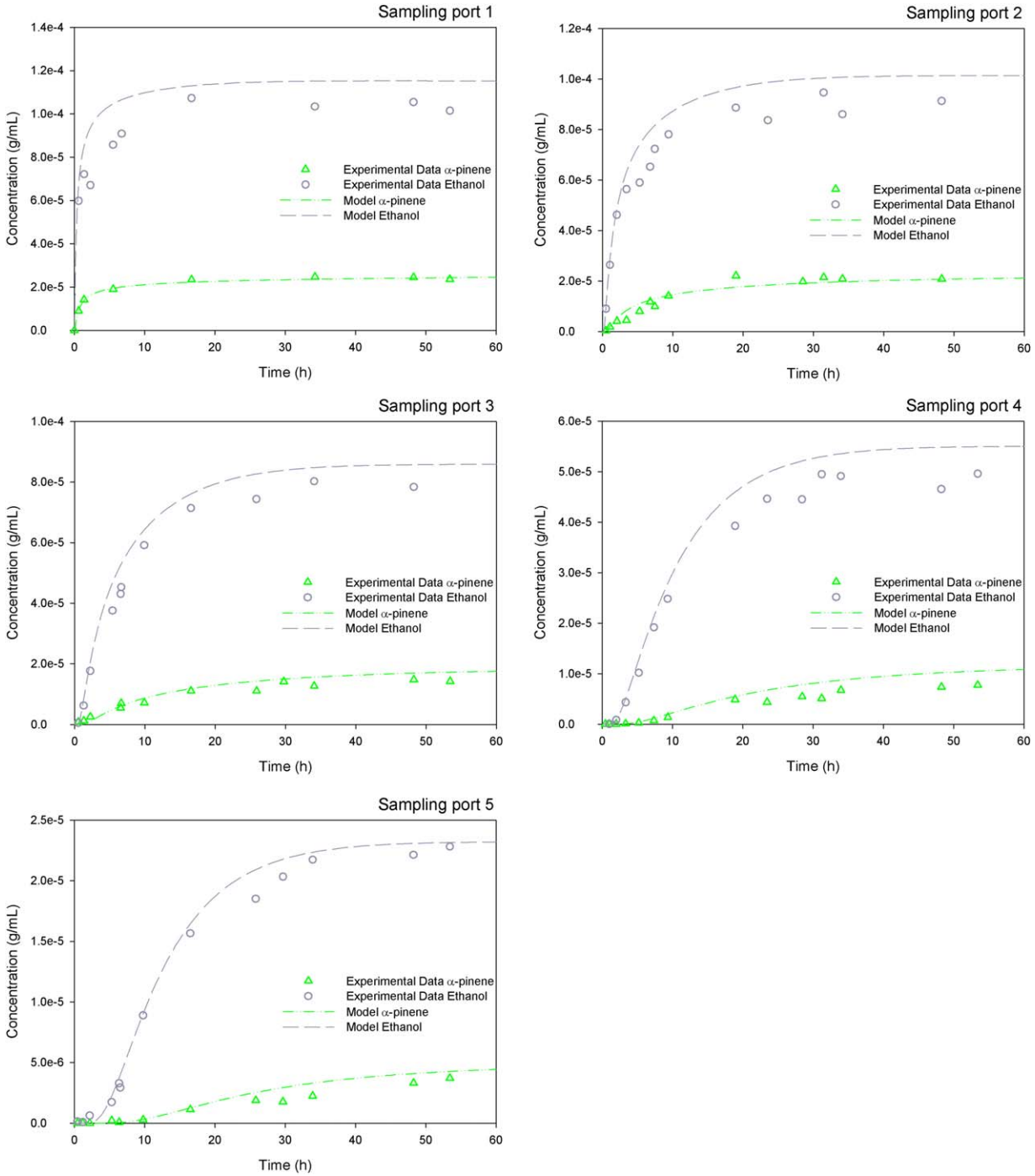

Figure 7. Experimental data (open symbols) and modeling (lines) for the diffusion of the binary mixture of ethanol + α-pinene in air measured at different heights from the source (different SPs).

[Color figure can be viewed in the online issue, which is available at wileyonlinelibrary.com.]

Table 6. Fragrance Chemicals, Weighed Masses, Moles and Mole Fractions (x_i) for the Composition of Quaternary Mixtures Q1 and Q2

	Q1			Q2		
Fragrance Chemical	Mass (g)	Mol	x_i	Mass (g)	Mol	x_i
α-pinene	1.04280	7.668×10^{-3}	0.37	0.91317	6.714×10^{-3}	0.27
Linalool	1.48824	9.664×10^{-3}	0.46	1.42235	9.236×10^{-3}	0.38
Tonalide	0.11263	4.434×10^{-4}	0.02	1.48217	5.835×10^{-3}	0.24
Ethanol	0.14634	3.181×10^{-3}	0.15	0.12369	2.689×10^{-3}	0.11

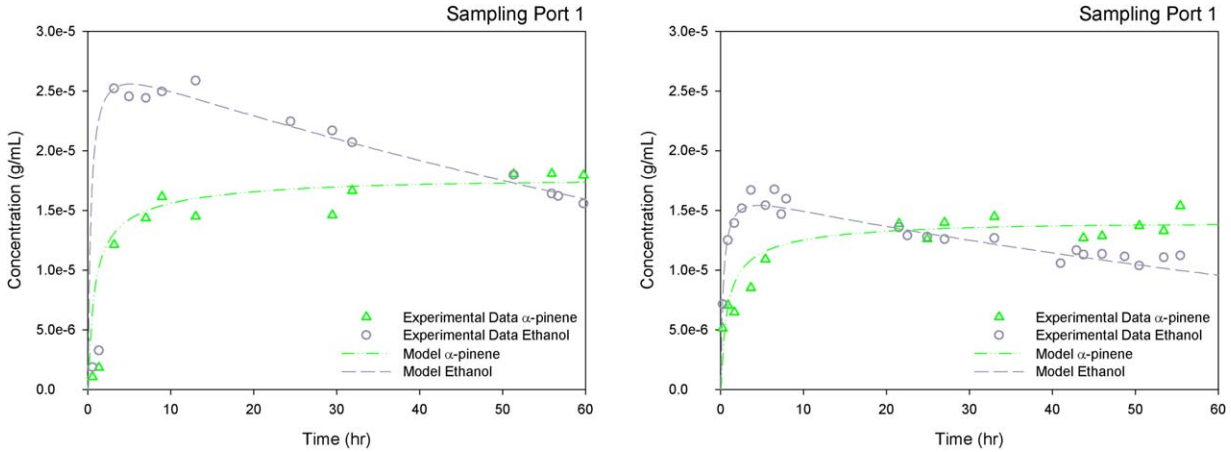

Figure 8. Diffusion profiles for ethanol and α-pinene in the quaternary mixtures Q1 (left) and Q2 (right) for sampling port 1.

[Color figure can be viewed in the online issue, which is available at wileyonlinelibrary.com.]

measured, either because their concentrations were below the detection limit or they were not quantitatively measured (e.g., tonalide, a fixative with an extremely low-vapor pressure).

For the results obtained in the release and diffusion of the multicomponent perfume mixture, it is possible to see, first, that our model describes well the propagation of the fragrance molecules inside the diffusion tube for all the cases that it could be measured. This means that the UNIFAC method used for the VLE together with our diffusion model are suitable for describing the evaporation and release of a complex mixture like this. Furthermore, the predicted diffusion coefficient fits very well with the experimental one in all cases. The ARDs for odorant concentrations were 9.2, 13.5, and 21.9% for ethanol, α-pinene, and limonene, respectively (see Table 5). The higher errors obtained for limonene are mainly due to sampling port P3, where larger deviations were observed. Concentration profiles are only shown for these three chemicals because the remaining ones presented extremely lower concentrations which were impossible to quantify with accuracy and reproducibility using our experimental technique and equipments. Their quantification in the gas phase is very difficult and would possibly require the use of different sampling procedures for increasing concentration of volatiles (e.g., solid-phase micro extraction) which would, in turn, change the equilibrium and diffusion conditions inside the tube. In our experiments, we have sampled 0.10 or 0.25 mL of gas phase in a control volume of 5 mL, thus not introducing significant disturbance in the system. It should be emphasized that, as the simulation results have confirmed the experimental data for the most volatile species, it is reasonable to extrapolate that our purely predictive model would fit the behavior of the other compounds.

Table 7. Fragrance Chemicals, Weighed Masses, Moles and Mole Fractions (x_i) for the Composition of the Multicomponent Perfume Mixture

Fragrance chemical	Note	Mass (g)	Mol	x_i
α-pinene	Top	0.0341	0.00025	0.0042
Limonene	Top	0.3276	0.00241	0.0405
Decanal	Top-to-middle	0.3325	0.00213	0.0359
Linalool	Middle	0.2021	0.00131	0.0221
Benzyl Acetate	Middle	0.2424	0.00162	0.0272
Geraniol	Middle	0.0116	0.00008	0.0013
2-Phenethyl Alcohol	Middle	0.0323	0.00026	0.0045
Cinnamic Alcohol	Base	0.0082	0.00006	0.0010
Tonalide	Base	0.0036	0.00001	0.0002
Ethanol	Solvent	1.7568	0.03816	0.6428
Deionized Water	Solvent	0.2353	0.01307	0.2203

Performance evaluation

Finally, the evaluation of fragrance performance is not complete if we do not translate odorant concentrations in air into odor perceptions. For that purpose, fragrance concentrations can be converted into odor intensities using Eq. 11, as previously discussed. From that point, it is possible to calculate odor intensities of each odorant and, thus, convert the concentration profiles (on the left side of Figure 9) into odor intensity profiles (right side of Figure 9). More important, the perceived odor intensity and character can be evaluated using Eq. 12 and, thus, map the predicted dominant odors over time and distance in a fragrance performance plot, as presented in Figure 10.

It can be seen from the performance plot in Figure 10 that the main character of the multicomponent mixture selected for this study evolves throughout time and distance from the source of release. The odor space is dominated by three fragrance chemicals (α-pinene, limonene, and decanal) as well as by the solvent (ethanol) depending on the time and distance variables. From a perfumery point of view, it is highly undesirable to formulate a fragrance that will smell strongly of ethanol because it is an irritant and not appreciated by customers. Accordingly, from our results, it was possible to observe that ethanol is the fastest component to evaporate (and also the most volatile), although it has a strong interaction with water, as previously reported.[18] Note, however, that as aforementioned, in a regular usage of a perfume there will be convection effects which will speed up ethanol dispersion, thus reducing its dominance in the performance plot (grey area).

The evaluation of the performance for this specific multicomponent mixture shows that the impact parameter is balanced between the ethanol/α-pinene pair, while α-pinene alone dominates the tenacity. If we move away from the source of release, it is seen that ethanol dominates the diffusion performance parameter, something that was expected because it presents one of the highest diffusion coefficients among all compounds. Finally, the binary pair α-pinene/

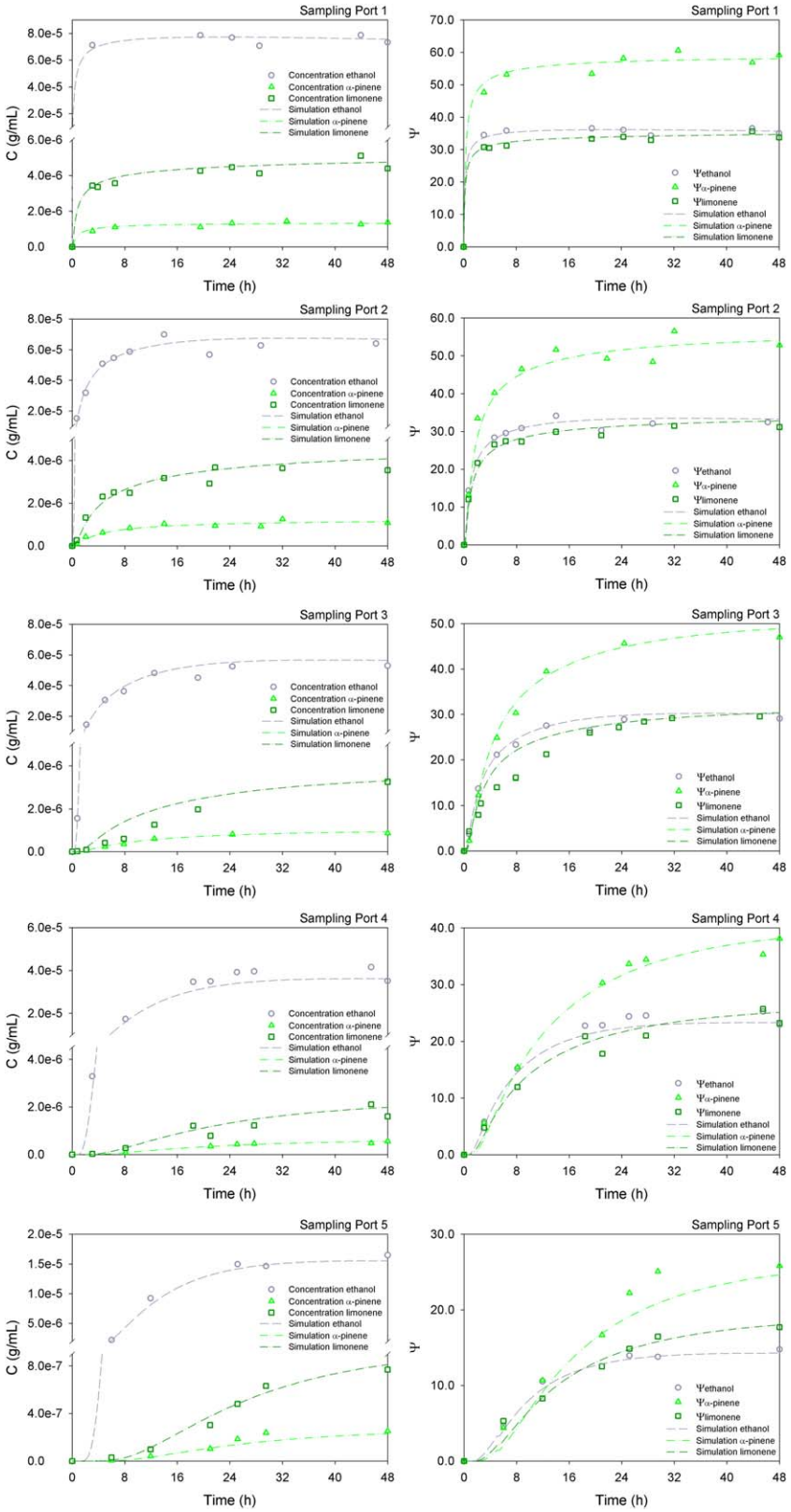

Figure 9. Diffusion profiles in terms of concentration (left) and odor intensities (right) for ethanol, α-pinene, and limonene in the multicomponent perfume mixture for the SPs.

[Color figure can be viewed in the online issue, which is available at wileyonlinelibrary.com.]

decanal dominates the volume performance parameter, depending on how far we are from the source.

In Figure 10, some experimental data points are also represented on the performance plot to establish a comparison between simulated odor intensities and those calculated from experimental vapor concentrations. It is seen that the predicted odor intensities are extremely close to experimental ones measured in specific points with an average deviation of

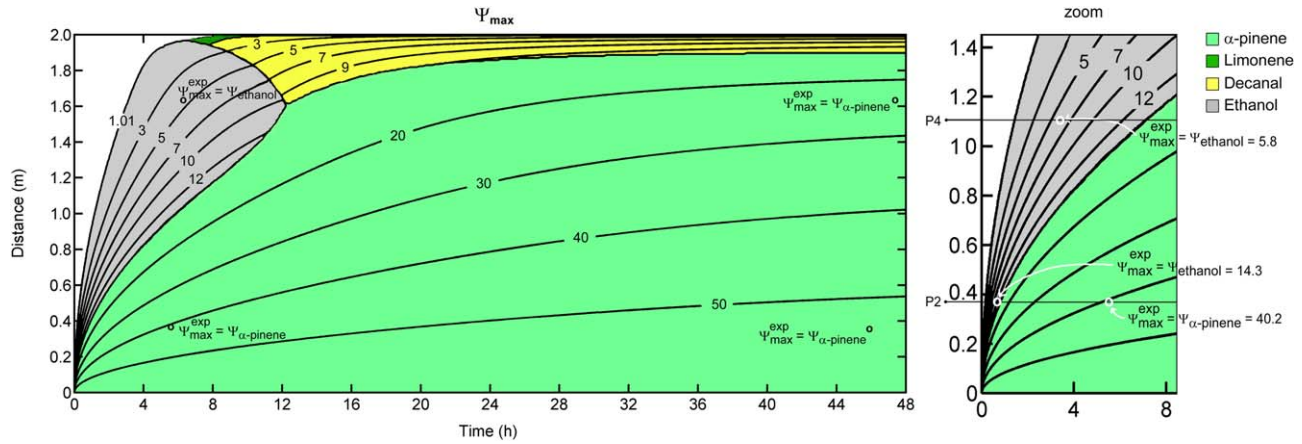

Figure 10. Fragrance performance plot for the multicomponent mixture, representing the dominant odorant over time and distance.

Odor iso-intensity lines are represented to show the relative odor intensities of the mixture in the different regions of the diagram. [Color figure can be viewed in the online issue, which is available at wileyonlinelibrary.com.]

6.3%. This is an outstanding result because it is known that only in the estimation of saturated vapor pressures we will find an error around 5%. This perspective can be better observed for multiple experimental data in Figure 11.

It was observed that the predicted dominant odor agreed in 95% of the times with the experimental one calculated from experimental headspace data points. For example, a point which is very close to a switch in dominant odor is seen in sampling port 2 for the experimental point taken at 0.7 h. This point resulted in $\Psi_{\text{ethanol}} = 14.3$ and $\Psi_{\alpha-\text{pinene}} = 13.3$, thus ethanol is more strongly perceived, and a similar behavior was also predicted from our model (see Figure 10). Furthermore, it was observed that only 2 (for a total of 40) experimental points did not agree with the predicted maximum odorant (in sampling port 3 at 0.78 h and sampling port 5 at 11.9 h). However, these two mismatches correspond to switching zones in the dominant odor, and it was even seen that two fragrance components had nearly the same odor intensity (for sampling port $3 - \Psi_{\text{ethanol}} = 3.8$ and $\Psi_{\text{limonene}} = 4.3$, for sampling port $5 - \Psi_{\text{ethanol}} = 10.5$ and $\Psi_{\alpha\text{-pinene}} = 10.7$). From this finding, it is also possible to conclude that the dominant odor is very well predicted, even in points where there is a switch in the dominant fragrance note. Consequently, our model that uses only estimated properties and is purely predictive proves a high accuracy. As a final remark, it should be said that although this predictive model (as happens with others) will probably never replace the human nose, it has shown to be a valuable tool in perfume design. The use of this type of model can help perfumers to reduce the number of trial-and-error formulations, consumption of perfumery raw materials and, ultimately, product's cost.

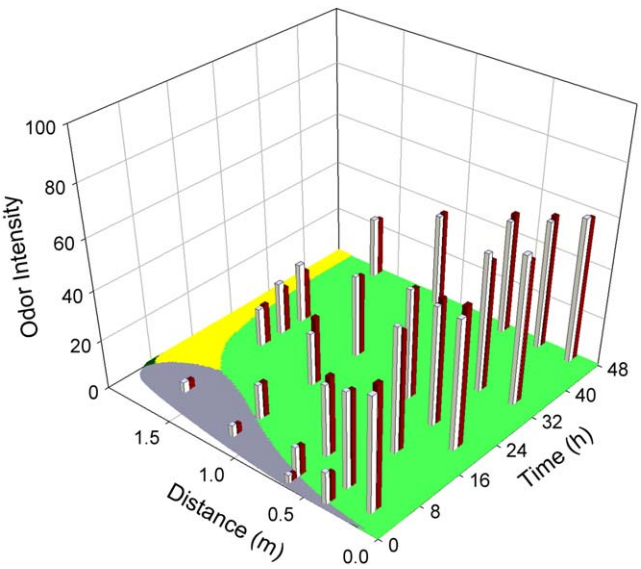

Figure 11. Comparison between the predicted (red bars) and experimental (white bars) odor intensities for the specific data points over time and distance.

[Color figure can be viewed in the online issue, which is available at wileyonlinelibrary.com.]

Conclusions

The odor profile of a multicomponent mixture of fragrances is the odor fingerprint of a perfume. It was observed from the results presented in this work that both odor intensity and odor character change with time and distance from the source. Consequently, it is straightforward to state that the performance of a perfume depends on the intrinsic properties of its constituents, but also on their molecular interactions in the liquid solution. Thus, the evaporation rate of each fragrance remains a function of mixture's initial composition (x_i), molecular interactions (activity coefficient, γ_i), and temperature (T) but it is simultaneously dependent on the physicochemical and psychological properties of fragrance chemicals (diffusivity, saturated vapor pressure, molecular weight, ODT, and power law exponent).

Moreover, it was seen that the relationship between the composition in the liquid and gas phases is difficult to predict at first sight, as the system of equations solved numerically is highly nonlinear. However, it is possible to say that ethanol and α-pinene were the components that evaporated faster for the mixtures tested, showing a significant decrease in the liquid composition during the first hours.

The experimental data measured for fragrance profiles over time and distance compared favorably with the model based on Fick's approach for diffusion when applied to pure

components like ethanol and α-pinene. Furthermore, our model also performed very well for binary, quaternary, and multicomponent mixtures of fragrance chemicals with an overall average relative deviation of 12.8% in 358 data points. In respect to this topic, it is important to highlight the following conclusions:

i. For single fragrance chemicals, steady-state concentrations were well predicted by our model, although the experimental error should not be forgotten.

ii. Predicted concentration profiles fitted well with the experimental data for initial times, showing that the estimated diffusion coefficients were suitable for this purpose.

iii. Diffusion of typical quaternary fragrance mixtures comprising three different fragrance notes and a solvent clearly showed the effect of the presence of a fixative: a good fitting of the model with the experimental data was observed, and this retention effect of tonalide on the most volatile components is correctly predicted.

iv. Release and propagation of a multicomponent perfume mixture was very well predicted from our model and validated with experimental data for the most volatile components. This is a great advance for fragrance design and performance as dealing with such a complex mixture is highly nonideal.

Another important conclusion to draw from this work is that it is possible to measure and predict the performance of a perfumed product using perfumery terminology and a theoretical model to assess the perceived odor over time and distance from the source. Note, however, that the combination of our models with real olfactory measurements performed by perfumers would be of great value for performance evaluation. Finally, it is likely that the art of perfumery involved in the formulation of the product will continue to play the key role in its definition and development process, but our predictive tool might help perfumers for a faster and cheaper design of new fragrances.

Acknowledgments

This work is partially supported by project PEst-C/EQB/LA0020/2011, financed by FEDER through COMPETE–Programa Operacional Factores de Competitividade and by FCT–Fundação para a Ciência e a Tecnologia. We acknowledge the contribution given from Ana C. Soares during some experimental work. O.R. acknowledges financial support of Programme Ciência 2007 (FCT). M.A.T. acknowledges his Postdoc. grant from FCT (SFRH/BPD/76645/2011).

Literature Cited

1. Cussler EL. *Diffusion: Mass Transfer in Fluids*, 3rd ed. Cambridge, UK: Cambridge University Press, 2007.
2. Calkin R, Jellinek S. *Perfumery: Practice and Principles*. New York: Wiley, 1994.
3. Gygax H, Koch H. The measurement of odours. *Chimia. Spec Issue Flavours Fragrances.* 2001;55:401–405.
4. Stora T, Eschera S, Morris A. The physicochemical basis of perfume performance in consumer products. *Chimia.* 2001;55:406–412.
5. Quellet C, Schudel M, Ringgenberg R. Flavors & Fragrance Delivery Systems. *Chimia.* 2001;55:421–428.
6. Kasting GB, Saiyasombati P. A physico-chemical properties based model for estimating evaporation and absorption rates of perfumes from skin. *Int J Cosmet Sci.* 2001;23:49–58.
7. Kasting GB, Saiyasombati P. Two stage kinetics analysis of fragrance evaporation and absorption from skin. *Int J Cosmet Sci.* 2003;25:235–243.
8. Heltovics G, Holland LAM, Warwick JM, Jenkins DM, Sutton KL, Pretswell EL, Shefferd AJP, Inventors. Methods and compositions for improved fragrancing of a surface. US Patent 2004/0097398 A12004 The Procter & Gamble Company, 2004.
9. Teixeira MA, Rodríguez O, Mata VG, Rodrigues AE. The diffusion of perfume mixtures and odor performance. *Chem Eng Sci.* 2009;64:2570–2589.
10. Mata VG, Gomes PB, Rodrigues AE. Engineering perfumes. *AlChE J.* 2005;51(10):2834–2852.
11. Fadel A, Turk R, Mudge G, Mattila J, Esteves J, Ranciato J, Inventors. Perfumes for rinse-off systems. US Patent 7,446,079 B22008.
12. Cortez-Pereira CS, Baby AR, Kaneko TM, Velasco MVR. Sensory approach to measure fragrance intensity on the skin. *J Sens Stud.* 2009;24(6):871–901.
13. Fadel A, Turk R, Mudge G, Sullivan D, Goberdhan V, Meo AD, Inventors. Malodor covering perfumery. US Patent 7,585,833 B22009.
14. Duprey RJH, Perring KD, Ness JN, Inventors; Quest International Services B.V., assignee. Perfume Compositions. US Patent 7,713,922 B22010.
15. Járvás G, Quellet C, Dallos A. COSMO-RS based CFD model for flat surface evaporation of non-ideal liquid mixtures. *Int J Heat Mass Transfer.* 2011;54 4630–4635.
16. Teixeira MA, Rodríguez O, Mata VG, Rodrigues AE. Perfumery quaternary diagrams for engineering perfumes. *AlChE J.* 2009;55(8):2171–2185.
17. Teixeira MA, Rodríguez O, Mota FL, Macedo EA, Rodrigues AE. Evaluation of group-contribution methods to predict VLE and odor intensity of fragrances. *Ind Eng Chem Res.* 2011;50:9390–9402.
18. Teixeira MA, Rodríguez O, Rodrigues AE. The perception of fragrance mixtures: A comparison of odor intensity models. *AlChE J.* 2010;56(4):1090–1106.
19. Teixeira MA, Rodrìguez O, Rodrigues AE. Odor detection & perception: an engineering perspective. In: *Advances in Environmental Research*, Chapter 1, Vol. 14. New York: NOVA Publishers, 2011.
20. Seidera WD, Widagdo S, Seader JD, Lewin DR. Perspectives on chemical product and process design. *Comput Chem Eng.* 2009;33:930–935.
21. Ottino JM. Chemical engineering in a complex world: Grand challenges, vast opportunities. *AlChE J.* 2011;57(7):1654–1668.
22. Hill M. Chemical product engineering – The third paradigm. *Comput Chem Eng.* 2009;33(5):947–953.
23. Cussler EL, Wagner A, Marchal-Heussler L. Designing chemical products requires more knowledge of perception. *AlChE J.* 2010;56(2):283–288.
24. Carles J. A method of creation in perfumery. *Soap Perfum Cosmet.* 1962;35:328–335.
25. Calkin R, Jellinek S. *Perfumery: Practice and Principles*. New York: Wiley, 1994.
26. Teixeira MA, Rodriguez O, Gomes P, Mata V, Rodrigues A. *Perfume Engineering: Design, Performance & Classification*. Oxford, UK: Elsevier, 2012.
27. Chemspider. Database of Chemical Structures and Property Predictions – Royal Society of Chemistry. [Database]. 2011. Available at: http://www.chemspider.com/Default.aspx. Accessed February 2011.
28. van Gemert LJ. *Compilations of Odour Threshold Values in Air, Water and other Media*. The Netherlands: Oliemans Punter & Partners BV: Houten, The Netherlands, 2003.
29. Devos M, Rouault J, Laffort P. *Standardized Olfactory Power Law Exponents*. Dijon, France: Editions Universitaires-Sciences, 2002.
30. Fuller EN, Schettler PD, Giddings JC. A new method for prediction of binary gas-phase diffusion coefficients. *Ind Eng Chem.* 1966;58(5):19–27.
31. Lee CY, Wilke CR. Measurements of vapor diffusion coefficient. *Ind Eng Chem.* 1954;46(11):2381–2387.
32. Heinzelmann FJ, Wasan DT, Wilke CR. Concentration profiles in a Stefan diffusion tube. *Ind Eng Chem Fundam.* 1965;4(1):55–61.
33. Kerkhof PJAM. New light on some old problems: Revisiting the Stefan tube, Graham's law, and the Bosanquet equation. *Ind Eng Chem Res.* 1997;36:915–922.
34. Whitaker S. Role of the species momentum equation in the analysis of the Stefan diffusion tube. *Ind Eng Chem Res.* 1991;30:978–983.
35. Bird R, Stewart W, Lightfoot E. *Transport Phenomena*, 2nd ed. Singapore: Wiley, 1960.

36. Poling B, Prausnitz JM, O'Connell J. *The Properties of Gases and Liquids*, 5th ed. New York: McGraw-Hill, 2004.
37. MathWorks. Partial Differential Equation Toolbox—ComsoLab MATLAB's Users Guide, 2002.
38. Shampine LF, Reichelt MW. The MATLAB ODE suite. New York: The MathWorks, 1996.
39. Chapman J. *MATLAB Programming for Engineers*. CA: Brooks Cole Publishing Company, 2000.
40. Chapra S, Canale, R. *Numerical Methods for Engineers: With Software and Programming Applications*, 4th ed. Boston, MA: McGraw Hill, 2002.
41. Nocedal J, Wright, S. *Numerical Optimization*. New York: Springer, 1999.
42. Stevens SS. On the psychological law. *Psychol Rev*. 1957;64(3):153–181.
43. Appell L. Physical foundations in perfumery—VIII. The minimum perceptible. *Am Perfum Cosmet*. 1969;84:45–50.
44. Laffort P, Dravnieks A. Several models of suprathreshold quantitative olfactory interaction in humans applied to binary, ternary and quaternary mixtures. *Chem Senses*. 1982;7(2):153–174.
45. Cain WS, Schiet FT, Olsson MJ, de Wijk RA. Comparison of models of odor interaction. *Chem Senses*. 1995;20:625–637.
46. Perry RH. *Perry's Chemical Engineers' Handbook*, 7th ed. New York: McGraw-Hill, 1997.
47. Bird R, Stewart W, Lightfoot E. *Transport Phenomena*, 2nd ed. New York: Wiley, 2002.
48. Taylor R, Krishna R. *Multicomponent Mass Transfer*. New York: Wiley, 1993.
49. Wesselingh JA, Krishna R. *Mass Transfer in Multicomponent Mixtures*. Delft, The Netherlands: Delft University Press, 2000.
50. Philibert J. One and a half century of diffusion: Fick, Einstein, before and beyond. *J Basic Principles Diffus Theory, Exp Appl. (Diffus Fundam)*. 2006;4:6.1–6.19.
51. Lugg GA. Diffusion coefficients of some organic and other vapors in air. *Anal Chem*. 1968;40(7):1072–1077.

Manuscript received Oct. 30, 2012, and revision received Feb. 18, 2013.